HIGH SPECTRAL RESOLUTION SPECTROSCOPY OF MARS FROM 2 TO 4 μm: SURFACE MINERALOGY AND THE ATMOSPHERE. Diana Blaney*[1] , David Glenar*[2], and Gordon Bjorker*[2], [1] NASA Jet Propulsion Laboratory, California Institute of Technology 4800 Grove Dr., MS 183-501. Pasadena, CA 91001, Email: Diana.Blaney@jpl.nasa.gov; [2] NASA Goddard Space Flight Center, Planetary Systems Branch, Code 693, Bldg 2, Rm 162, Greenbelt, MD 20771, Email: David.Glenar@gsfc.nasa.gov, Gordon.L.Bjoraker@gsfc.nasa.gov. * Visiting Astronomers at the NASA Infrared Telescope Facility.

Introduction: The composition of the Martian surface and atmosphere on a global scale has been discovered in great part from spectroscopic measurements in the visible through infrared. Spectroscopic observations on Mars however require careful analysis from both atmospheric and mineralogical perspectives.

The 2-4 μm region contains diagnostic absorption features indicative of water such as the 3 μm bound water band and cation-0H stretches between 2-2.5 μm. Carbonate minerals also have absorption features in these wavelength range. However, this wavelength region also has atmospheric signatures from CO, CO_2, water vapor, clouds, and atmospheric dust that complicate direct mineralogical interpretations. Several absorption features have been identified in the in the 2.0 - 2.5 μm (e.g. Clark et al. 1990, Murchie et al. 1993, Bell et al. 1994) at moderate resolution. These features, while intriguing, are weak, narrow, and frequently at the edge of instrumental and observational limits.

Spectroscopic observations at high spectral resolutions ($\lambda/\lambda\Delta > 800$) can aid in the separation of weak surface and atmospheric absorptions that at lower resolution overlap. This paper focuses on understanding the atmospheric spectral signatures so that the underlying surface mineralogy can be understood.

Figure 1. Long slit drift-scan geometry during the 1999 KPNO observations

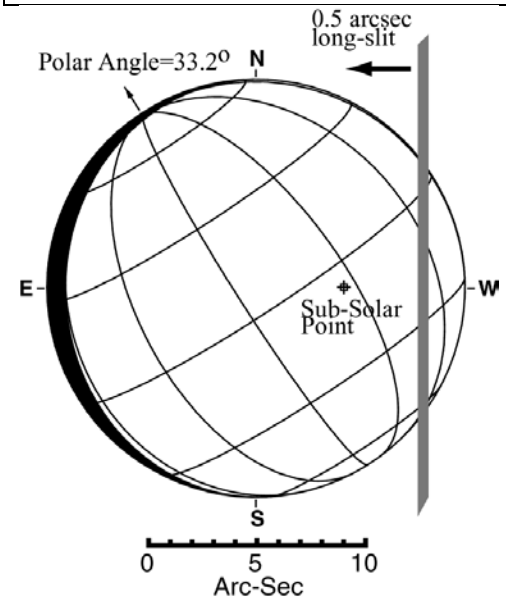

Observations: Imaging spectroscopy observations of Mars from 2 to 4.12 μm at high spectral resolution ($\lambda/\lambda\Delta \sim 800$-2300) were collected in April 1999 using the cryogenic long slit spectrometer at the Kitt Peak National Observatory 2.2 m telescope and in July 2001 using SpeX at the NASA Infrared Telescope Facility. The 1999 data have been used to model the cloud optical depth, particle sizes, and ice aerosol content of the aphelion cloud belt and to monitor diurnal changes in clouds (Glenar *et al.* 2003). Preliminary analysis of the atmospheric dust, clouds, and ice of the 2001 data has also been undertaken (Glenar et al. 2002)

A high spectral resolution image cube is created by allowing the spectrometer slit to slowly drift across the disk, while recording a continuous stream of 1D spectral x 1D spatial images. Customary processing steps (flatfield, sky subtraction, photometric corrections and wavelength calibration using lamp or atmospheric features) are applied to each slit spectrum. Figure 1 shows an example drift scan. This example shows the slit motion and Mars aspect geometry during the July 14, 2001 SpeX observation. Slit is oriented celestial north-south and drifts west to east on the sky. Drift rate and spectrum coadd rates are chosen so that there are two spectral records per 0.5 arcsec slit width (Nyquist sampling). During a sequence, the telescope synchronously nods north-south to achieve careful sky-subtraction. The series of spectral images is reformatted into a spectral image cube. During the drift scan sequence, a boresighted guide camera acquires a continuous time-tagged image series. This is used later on to register each slit image in x and y, using a disk centroiding algorithm.

The influence of dust and clouds must be fully considered in spectroscopic analysis of the surface. Physical and diurnal properties of water ice clouds can be derived from this data as discussed below, as can the properties of atmospheric dust (e.g., optical depth and single scattering albedo). Finally, once the behavior of dust and clouds is understood, surface mineralogy can be investigated.

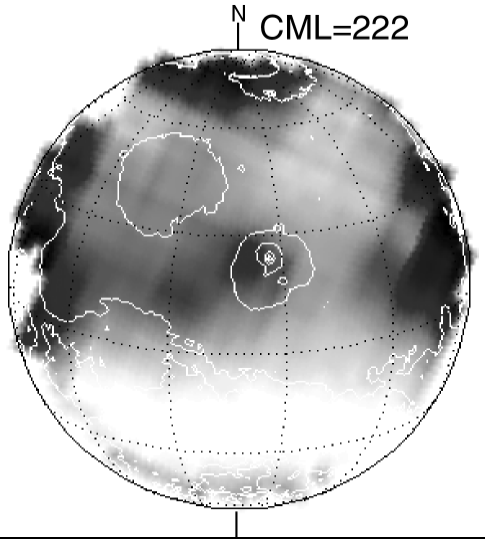

Figure 2. Three μm band depth map (one of 6) showing ice cloud opacity in a qualitative sense. Dark features near disk center show clouds immediately to the west of Elysium Mons. Other low latitude features arise from the diffuse aphelion cloud belt, and higher latitude features from the 3 μm hydration band

Figure 2 and 3 show the distribution and some properties of aphelion season clouds (Ls=130), from L-band image cubes acquired in April '99. Figure 2 shows a map of cloud optical depth obtained from one image cube, albeit poorly represented in this black and white figure. Dark represents larger cloud opacity. Prominent in this map (near center) is an orographic cloud which is just beginning to form on the west flank of Elysium Mons, at about 12:00 LST. Additional features at other positions arise from the diffuse, north tropical cloud band, as well as the spectral influence of the 3 micron surface hydration band, which shows up at higher latitudes. The local time evolution of the Elysium Mons cloud was analyzed quantitatively by fitting the measured cloud spectra from all six image cubes (spanning ~ 5 hours) to scattering models (Glenar et al. 2003). As shown in Figure 3, cloud thickness is initially indicative of morning cloud activity (c.f., Colaprete et al. 1999), followed by a decline in optical depth, and once again, prominent cloud growth due to afternoon convection and condensation in the cold aphelion atmosphere (Clancy et al. 1996).

The 2001 IRTF measurements were acquired at Ls=195, coincidentally just after the onset and initial growth of the large, early-season dust storm 2001A (Smith et al., 2002). Spectral image data acquired in K-band (Figure 4) show the effect of dust on the strength of the 2 micron atmospheric CO_2 absorption band. Increased dust opacity in the southern hemisphere suppresses the depth of this band, mostly because of the effect of dust scattering. Radiative transfer models incorporating scattering, combined with these observations can be used to estimate dust optical depth and also constrain the dust single scattering albedo, which is poorly known at these wavelengths (Clancy et al. 1995). Dotted lines in these plots show the results of scattering model calculations (DISORT, Stamnes et al. 1988) which crudely approximate the observations. Newly available dust RT parameters derived from MGS measurements of emission phase function, were provided for these calculations by Wolff and Clancy (personal communication). Such results are sensitive not only to dust optical depth, but also to the assumed dust vertical distribution.

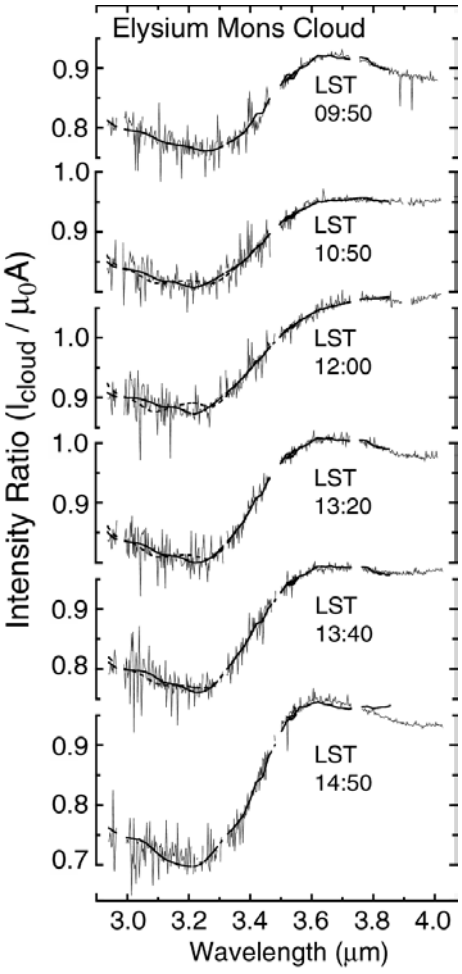

Figure 3. Local time evolution of the Elysium Mons cloud spectral shape. Derived optical depth (τ at 3.2 μm) is indicated at each time step.

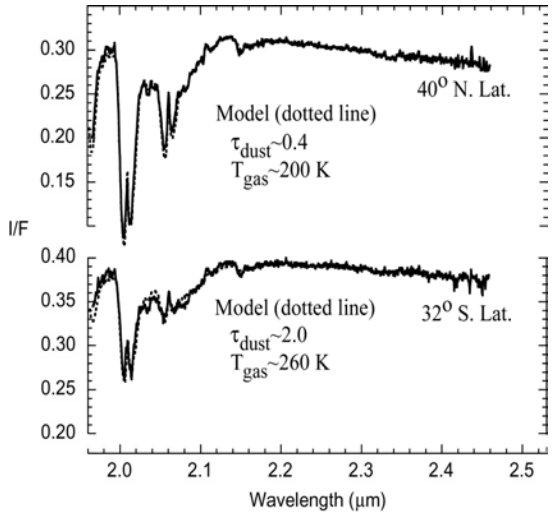

Figure 4. K-band spectra along the central meridian, in the northern (top) and southern (bottom) hemispheres during the global dust storm 2001A. Dotted lines show model comparison spectra.

Figure 5 shows a map of atmospheric CO2 band depth, which is a reliable (but qualitative) indicator of dust optical depth. The dark region at north latitudes, near 0 deg longitude indicates a minimum in dust optical depth. This partial void was also observed by MGS TES at about the same Ls (M. Smith, personal communication) and was later filled as the dust storm evolved.

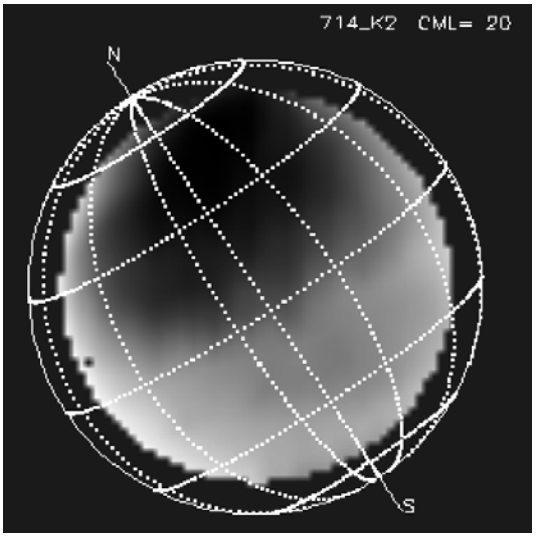

Figure 5. Atmospheric CO2 band depth map. This provides a qualitative, inverse measure of dust optical depth. Bright in this figure indicates larger dust optical depth.

The detailed modeling of cloud properties (Glenar et al 2003) permits us to now identify regions where the atmosphere is clear and to look for variations in the 3 μm bound water band and for Cation-OH stretches on the Martian surface independent of possible clouds. Similarly, we can use indications of dust opacity in the 2 μm carbon dioxide gas band to identify clear regions that are minimally affected by the 2001 dust storm. The high spectral resolution also enables the clean identification of atmospheric features, solar lines, residual telluric absorptions, and weak surface features.

Weathered Basalt or Andesite? Banfield *et al.* 2000 mapped the surface of Mars using data from the Mars Global Surveyor Thermal Emission Spectrometer (TES). They identified two distinctive surface spectral signatures in the low albedo regions. Modeling and comparison to terrestrial igneous materials showed that Type I material (older and located in the Southern highlands) was basaltic in nature while Type II (located in the younger Northern plains) was of andseitic composition. Wyatt and McSween 2002 put forth an alternative interpretation for the Type II unit as a weakly altered basalt due to: similarities between the spectral characteristics of clays and high silica glass; geochemical arguments against the production of large volumes of andesite given Mars's geologic history; and comparisons between the location of Type II material and proposed standing bodies of water in the Northern plains of Mars.

Wavelengths between 2-4 μm have diagnostic absorption features indicative of water such as the 3 μm bound water band and cation-0H stretches between 2-2.5 μm. The large areal extent of the Type I and Type II units means that ground-based observations in this wavelength range could provide additional information on composition.

The 2001 IRTF SPeX data was used to identify Type II material based on observational geometry and evaluation of dust opacity. An represent spectra of this region was extracted using a 3x3 pixel box—shown in red in Figure 6. This represents ~0.9 arc seconds area of the disc and is consistent with our spatial resolution. Note that there are clear albedo contrasts at this wavelength in spite of the dust storm. Figure 7 shows the extracted spectra and the spectra of montmorillonite (a clay). No distinctive cation-OH stretches were seen, indicating that well crystalline clays are beneath our detection limits at this location. No evidence for carbonates is observed. The fine structure seen in the spectra are due to absorptions in the Martian atmosphere (including dust, e.g. figure 4) and solar spectral features. At this spectral resolution mineralogical absorption features are much broader than those observed in the spectra.

The 1999 KPNO data was used to identify a region of Type II material in our dataset between 30° and 50°N latitude and 260° - 280°W longitude. The spec-

tra show a clear 3 μm bound water band. The attempt to identify Type I regions that were cloud free in our data set was problematic due to its association with volcanoes (which develop orographic clouds) and to its equatorial distribution**,** which is affected by the aphelion cloud belt. Careful comparison of the Type II material to the Type I basaltic unit and the Martian bright regions in the future may permit an assessment of the relative hydration state of the Type II materials and help resolve this debate. However, detailed modeling of the spectra will be required and other effects such as grain size, cementation, and viewing geometry need to be assessed.

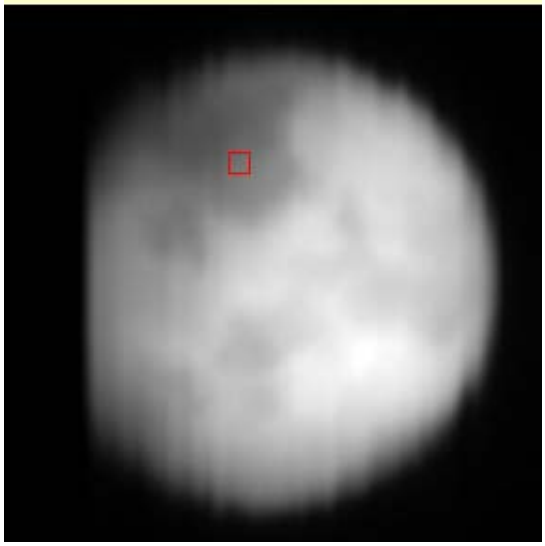

Figure 6. Location of the spectrum shown in figure 7.

This work is supported by the NASA Planetary Astronomy Program, under RTOP 344-32-51-02 and was performed at the NASA Jet Propulsion Laboratory, California Institute of Technonlogy and at the NASA Goddard Space Flight Center.

References: Banfield. J. L., V. E. Hamilton, P. R. Christensen, A Global View of Martian Surface Compositions from MGS-TES, Science, 287. 1626-1630, 2000.

Bell et al., Spectroscopy of Mars from 2.04 to 2.44 μm during the 1993 Opposition: Absolute Calibration and Atmospheric vs. Mineralogical Origin of Narrow Absorption Features, Icarus, 111, 106-123, 1994.

Clancy, R.T. and 8 coauthors, Water vapor saturation at low altitudes around Mars aphelion: A key to Mars climate?, Icarus 122, 36-62, 1996.

Clancy, R. T., S. W. Lee, G. R. Gladstone, W. W. McMillan and T. Roush, A new model for Mars atmospheric dust based upon analysis of ultraviolet through infrared observations from Mariner 9, Viking and Phobos, J. Geophys Res. 100, 5251-5263, 1995.

Clark, R.N., et al., J. Geophys. Res., High resolution reflectance spectra of Mars in the 2.3 μm region: Evidence for the mineral scapolite, 95, 14463-14480, 1990.

Colaprete, A., O. B. Toon and J. A. Magalhaes, Cloud formation under Mars Pathfinder conditions, J. Geophys. Res. 104, 9043-9053, 1999

Glenar R., D.A. E. Samuelson, J. C. Pearl, G. L. Bjoraker, and D. L. Blaney, Mars Polar Volatiles: IR Spectral Mapping Results from the Oppositions of 1999 (Ls=130) and 2001 (Ls=182,195), Bulletin of the American Astronomical Society, 34, 3, 2002. (DPS Abstract 15.23)

Glenar, D.A., R.E. Samuelson, J.C. Pearl, G.L. Bjoraker and D. Blaney, Spectral Imaging of martian water ice clouds and their diurnal behavior during the 1999 aphelion season (Ls=130^{o}), Icarus 161, 297-318, 2003.

Bell et al., Spectroscopy of Mars from 2.04 to 2.44 μm during the 1993 Opposition: Absolute Calibration and Atmospheric vs. Mineralogic Origin of Narrow Absorption Features, Icarus, 111, 106-123, 1994.

Smith M. D., R. J. Conrath, J. C. Pearl, and P. R. Christensen Thermal Emission Spectrometer observations of Martian planet-encircling dust storm 2001A, Icarus, 157 (1): 259-263 2002.

Salisbury, J. W., Walter, L. S., Vergo, N., and D'Aria, D. M., Infrared (2.1- 25 micrometers) Spectra of Minerals: Johns Hopkins University Press, 294 pp., 1991.

Stamnes, K., S. C. Tsay, W. Wiscombe and K. Jayaweera, Numerically stable algorithm for discrete-ordinate-method radiative transfer in multiple scattering and emitting layered media, Appl. Opt. 27, 2502-2509, 1988.

Smith, M. D., B. J. Conrath, J. C. Pearl and P. R. Christensen, Thermal emission spectrometer observations of Martian planet-encircling dust storm 2001A, Icarus 157, 259-263, 2002.

Wyatt, M. B. and H. Y. McSween, Spectral evidence for weathered basalt as an alternative to andesite in the northern lowlands of Mars, Nature, 417, 263 – 266,2002

Figure 7. Type II material between 2-2.5 μm and an example clay mineral, montmorillonite.